

Specific and Nonhepatotoxic Degradation of Nuclear Hepatitis B Virus cccDNA

Julie Lucifora,^{1,2*} Yuchen Xia,^{1*} Florian Reisinger,¹ Ke Zhang,¹ Daniela Stadler,¹ Xiaoming Cheng,¹ Martin F. Sprinzl,^{1,3} Herwig Koppensteiner,¹ Zuzanna Makowska,⁴ Tassilo Volz,⁵ Caroline Remouchamps,⁶ Wen-Min Chou,¹ Wolfgang E. Thasler,⁷ Norbert Hüser,⁸ David Durantel,⁹ T. Jake Liang,¹⁰ Carsten Münk,¹¹ Markus H. Heim,⁴ Jeffrey L. Browning,¹² Emmanuel Dejudin,⁶ Maura Dandri,^{2,5} Michael Schindler,¹ Mathias Heikenwalder,^{1,††} Ulrike Protzer^{1,2,††}

Current antiviral agents can control but not eliminate hepatitis B virus (HBV), because HBV establishes a stable nuclear covalently closed circular DNA (cccDNA). Interferon- α treatment can clear HBV but is limited by systemic side effects. We describe how interferon- α can induce specific degradation of the nuclear viral DNA without hepatotoxicity and propose lymphotoxin- β receptor activation as a therapeutic alternative. Interferon- α and lymphotoxin- β receptor activation up-regulated APOBEC3A and APOBEC3B cytidine deaminases, respectively, in HBV-infected cells, primary hepatocytes, and human liver needle biopsies. HBV core protein mediated the interaction with nuclear cccDNA, resulting in cytidine deamination, apurinic/aprimidinic site formation, and finally cccDNA degradation that prevented HBV reactivation. Genomic DNA was not affected. Thus, inducing nuclear deaminases—for example, by lymphotoxin- β receptor activation—allows the development of new therapeutics that, in combination with existing antivirals, may cure hepatitis B.

Hepatitis B virus (HBV) infection remains a major public health threat, with more than 350 million humans chronically infected worldwide at risk of developing end-stage liver disease and hepatocellular carcinoma. Each year, more than 600,000 people die from the consequences of chronic HBV infection. A prophylactic vaccine has been available for hepatitis B for almost 30 years, but the overall number of chronic infections remains high.

HBV is a small, enveloped DNA virus replicating via an RNA intermediate. The encapsidated viral genome consists of a 3.2-kb partially double-stranded relaxed circular DNA (rcDNA) molecule. The virus has optimized its life cycle for

long-term persistence in the liver (1). Upon translocation to the nucleus, the rcDNA genome is converted into a covalently closed circular DNA (cccDNA), which serves as the template for viral transcription and secures HBV persistence. Nucleoside or nucleotide analogs are efficient antivirals but only control and do not cure HBV infection owing to the persistence of HBV cccDNA. Therefore, long-term treatment is required, which is expensive and may lead to concomitant resistance (2). Interferon (IFN)- α is licensed for hepatitis B therapy, and treatment with this cytokine can result in virus clearance in a proportion of patients; however, its efficacy is limited and high doses are not tolerated (3). Thus, efficient and nontoxic elimination of cccDNA in hepatocytes is a major goal of HBV research.

Using animal models, it has been shown that HBV replication—in particular, the cccDNA content of the liver—can be affected by noncytotoxic mechanisms involving cytokines such as interferons and tumor necrosis factor (TNF), which influence RNA and capsid stability (4–7). Here, we describe an antiviral mechanism that interferes with cccDNA stability and is distinct from influences of antiviral cytokines on cccDNA activity (8).

High-Dose IFN- α Leads to cccDNA Degradation in HBV-Infected Hepatocytes

IFN- α is known to exert transcriptional, post-transcriptional, and epigenetic antiviral effects on HBV (8–12). To study the effect of IFN- α on HBV cccDNA, we used HBV-infected, differentiated HepaRG (dHepaRG) cells and primary human hepatocytes (PHHs). These are human cell types susceptible to HBV infection (13, 14) and responsive to IFN- α treatment in vitro (fig. S1A). IFN- α treatment did not lead to detectable

hepatotoxicity, even at very high doses (fig. S1B). Treating dHepaRG cells with IFN- α (500 or 1000 IU/ml) controlled HBV-DNA synthesis as efficiently as the nucleoside analog lamivudine (LAM) at 0.5 μ M (5 times the median effective concentration, EC₅₀). IFN- α , however, unlike LAM, also significantly reduced expression of HBV-RNA and hepatitis B surface (HBsAg) and e (HBeAg) antigens (Fig. 1A and fig. S1C).

In patients, interruption of LAM treatment results in a rebound of HBV replication (2). Using IFN- α , we observed only a partial rebound, or none at all, in HBV-infected dHepaRG cells after treatment cessation (Fig. 1A). Because dHepaRG cells do not allow virus spread, reduction of HBeAg and the lack of rebound indicated an effect of IFN- α on the established HBV cccDNA transcription template separate from the known antiviral effects on viral replication (14). By cccDNA-specific quantitative polymerase chain reaction (qPCR), we determined an 80% reduction of cccDNA after 10 days of treatment (Fig. 1B). Reduction of cccDNA was confirmed by Southern blot analysis (fig. S1D) and was dose-dependent (fig. S1E). cccDNA reduction could be induced at any time point (Fig. 1C) and persisted over time (Fig. 1, A and C). The effect was corroborated in HBV-infected PHHs (Fig. 1D). In contrast to IFN- α , LAM and the even more potent nucleoside analog entecavir (ETV) at very high doses (0.5 μ M; 1000 times EC₅₀) only inhibited reverse transcription, and thus HBV replication, but not viral persistence (Fig. 1E). Pretreatment with ETV did not enhance the effect of IFN- α (Fig. 1F), indicating that IFN- α induces the decay of established HBV cccDNA. Because the doses of IFN- α used to achieve this effect were high, we screened for other cytokines showing similar antiviral effects at moderate doses.

LT β R Activation Controls HBV and Leads to cccDNA Degradation in HBV-Infected Cells

IFN- γ and TNF- α are known to control HBV in a noncytotoxic fashion (4, 7) but cannot be used as therapeutics because they cause severe side effects. We tested the effect of lymphotoxin (LT) β receptor (LT β R) activation as an alternative therapeutic option. The TNF superfamily members LT α , LT β , and CD258 are the physiological ligands for LT β R and activate either inflammatory or anti-inflammatory pathways or induce apoptosis (15). Like hepatocytes (16), dHepaRG (14) and HepG2-H1.3 cells permit HBV replication (17) and express LT β R (fig. S2, A and B). To activate LT β R, we used a superagonistic tetravalent bispecific antibody (BS1) and a bivalent anti-LT β R monoclonal antibody (CBE11) (18, 19). As expected, LT β R agonists activated canonical (20) and noncanonical nuclear factor κ B (NF- κ B) pathways to trigger p100 cleavage (fig. S2C), RelA phosphorylation (fig. S2D), nuclear RelB and RelA translocation (fig. S2, E and F), and up-regulation of known target genes (fig. S2G) without causing any detectable hepatocytotoxicity (fig. S2H).

¹Institute of Virology, Technische Universität München—Helmholtz Zentrum München, 81675 Munich, Germany.

²German Center for Infection Research (DZIF), Munich and Hamburg sites, Germany. ³1st Medical Department, University Hospital Mainz, 55131 Mainz, Germany. ⁴Department of Biomedicine, University Hospital Basel, 4031 Basel, Switzerland.

⁵Department of Internal Medicine, University Medical Center Hamburg-Eppendorf, 20246 Hamburg, Germany. ⁶GIGA-Research Laboratory of Molecular Immunology and Signal Transduction, University of Liège, 4000 Liège, Belgium. ⁷Department of General, Visceral, Transplantation, Vascular and Thoracic Surgery, Grosshadern Hospital, Ludwig Maximilians University, 81377 Munich, Germany. ⁸Department of Surgery, University Hospital Rechts der Isar, Technische Universität München, 85748 Munich, Germany. ⁹INSERM U1052, CNRS UMR 5286, Cancer Research Center of Lyon, University of Lyon, LabEx DEVweCAN, 69007 Lyon, France. ¹⁰Liver Diseases Branch, National Institute of Diabetes and Digestive and Kidney Diseases, Bethesda, MD 20892, USA. ¹¹Clinic for Gastroenterology, Hepatology and Infectiology, Medical Faculty, Heinrich-Heine University, 40225 Düsseldorf, Germany. ¹²Department of Immunobiology, Biogen Idec, Cambridge, MA 02142, USA.

*These authors contributed equally to this work.

†Corresponding author. E-mail: protzer@tum.de (U.P.); heikenwalder@helmholtz-muenchen.de (M.H.)

††These authors contributed equally to this work.

To test the effect of LTβR activation on HBV infection, we treated dHepaRG cells with BS1 for 12 days starting 24 hours before HBV infection. LTβR activation decreased levels of all HBV markers, including cccDNA, by ~90% without toxicity (Fig. 2A). The antiviral effect was highly potent, with an EC₅₀ of ~0.01 μg/ml (fig. S3A). Inhibition of apoptosis did not alter antiviral activity (fig. S4). Neither IFN-β nor representative IFN-stimulated genes were up-regulated upon BS1 treatment (fig. S2G), and antiviral activity was independent of IFN induction (fig. S5).

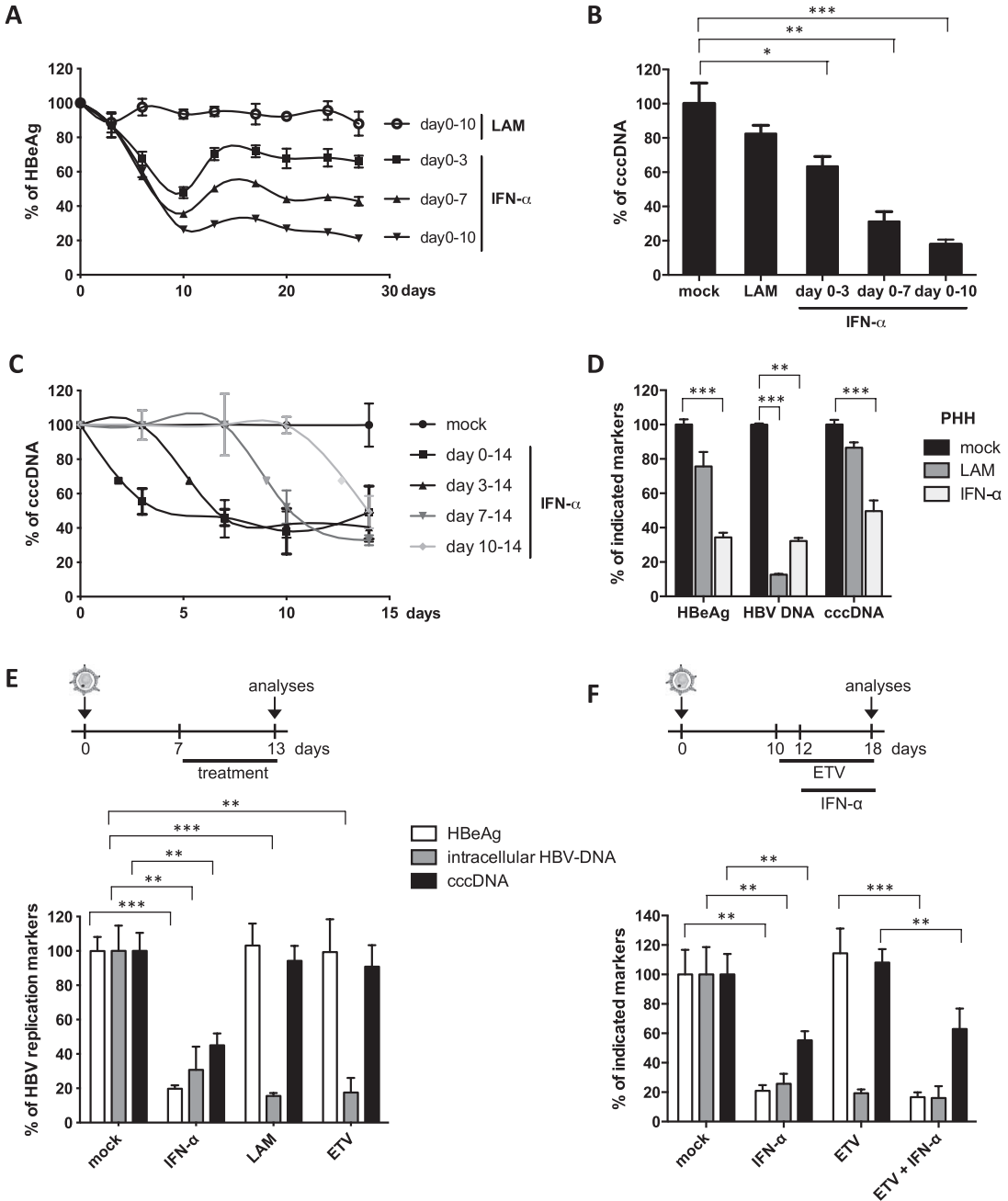
In vivo, activation of the murine LTβR by systemic application of an agonistic antibody (ACH6) induced RelA and RelB nuclear trans-

location in hepatocytes of HBV-transgenic mice (fig. S6A) and reduced HBV viremia (fig. S6B), HBV RNA (fig. S6C), and HBV core (HBc) protein expression in the liver (fig. S6, D and E). Neither signs of hepatocyte apoptosis (fig. S6F) nor elevation of aminotransferases (ALT) (fig. S6G, right panel) were observed, indicating good in vivo tolerability of LTβR activation. Because HBV-transgenic mice do not establish HBV cccDNA, this indicated additional antiviral effects of LTβR activation on HBV RNA transcription or stability. Accordingly, discontinuation of LTβR activation induced an immediate, strong rebound of HBV replication (fig. S6G).

To investigate whether LTβR activation would affect established HBV cccDNA in the context

of a persistent infection and prevent HBV reactivation, we treated dHepaRG cells with LTβR agonists BS1 or CBE11 when a stable, nuclear cccDNA pool had established. All HBV markers, including HBV cccDNA, were reduced upon LTβR activation in HBV-infected dHepaRG cells (Fig. 2, B and C, and fig. S3) as well as in stably transfected HepG2-H1.3 cells containing high levels of cccDNA (Fig. 2C). In HBV-infected PHHs, LTβR agonization reduced HBV cccDNA, HBeAg secretion, and—most effectively—HBV-DNA replication (Fig. 2D). cccDNA degradation was more effective (up to 95%) when treatment was prolonged (fig. S3, C and D). Treatment interruption for 10 days was almost as efficient as continuous treatment (fig. S3C), indicating that LTβR agonists

Fig. 1. Degradation of cccDNA in IFN-α-treated HepaRG cells and primary human hepatocytes. (A, B, C, E, and F) HBV-infected dHepaRG cells were treated with IFN-α at day 10 post-infection (dpi). Different regimens of treatment were applied as indicated. (D) HBV-infected PHHs were treated with IFN-α at dpi 3 for 13 days. Levels of HBeAg, total intracellular DNA, and cccDNA are given relative to mock-treated cells. LAM, lamivudine; ETV, entecavir. Data are means ± SD of replicates from independent experiments and were analyzed by *t* test. **P* < 0.05, ***P* < 0.01, ****P* < 0.001.



induce a persistent antiviral effect. In contrast to LAM treatment, no rebound of HBV replication was observed when BS1 treatment stopped (Fig. 2E). Hence, LT β R activation not only suppressed HBV replication but also caused nuclear cccDNA degradation, which is needed to achieve virus elimination.

LT β R Activation and IFN- α Treatment Induce Deamination and Apurinic/Apyrimidinic (AP) Site Formation in cccDNA

To investigate whether cccDNA degradation upon LT β R activation or IFN- α treatment was a result of DNA damage, we examined cccDNA deamination by differential DNA denaturation PCR (3D-PCR) (21). Lower denaturing temperatures were sufficient for cccDNA amplification from HBV-infected dHepaRG cells and for PHHs treated with IFN- α or BS1, compared with denaturing temperatures needed to amplify cccDNA from untreated, LAM-treated, or ETV-treated cells (Fig. 3A and fig. S7, C and D). Using a cocktail of recombinant proteins containing all enzymes necessary for DNA repair, we could reverse the denaturation of cccDNA (Fig. 3A, lower panels). The fact that the denaturation temperatures of mock-, LAM-, and ETV-treated cells also shifted

indicated that this modification of HBV cccDNA existed even without exposure to exogenous drugs. Deamination of cccDNA (Fig. 3A, right panel) and a drop in cccDNA levels after treatment with CBE11 (table S1) were confirmed in vivo in human liver chimeric uPA-SCID mice infected with HBV. Sequencing analyses showed that G \rightarrow A transitions occurred under treatment (Fig. 3B and fig. S7, A and B), indicating deamination of cytidines to uridine in the HBV cccDNA minus strand. At lower denaturation temperatures, G \rightarrow A transitions became more obvious (Fig. 3C and fig. S7A). These data showed that both LT β R activation and IFN- α treatment led to cccDNA deamination in vitro and in vivo, and help to explain the G \rightarrow A hypermutation observed in patient samples (21).

Neither deamination nor mutations of genomic DNA were observed by 3D-PCR (fig. S8A) or by deep sequencing of selected housekeeping genes or of IFN and LT β R target genes (fig. S8B). This finding indicated that DNA modifications were specifically targeted to viral cccDNA.

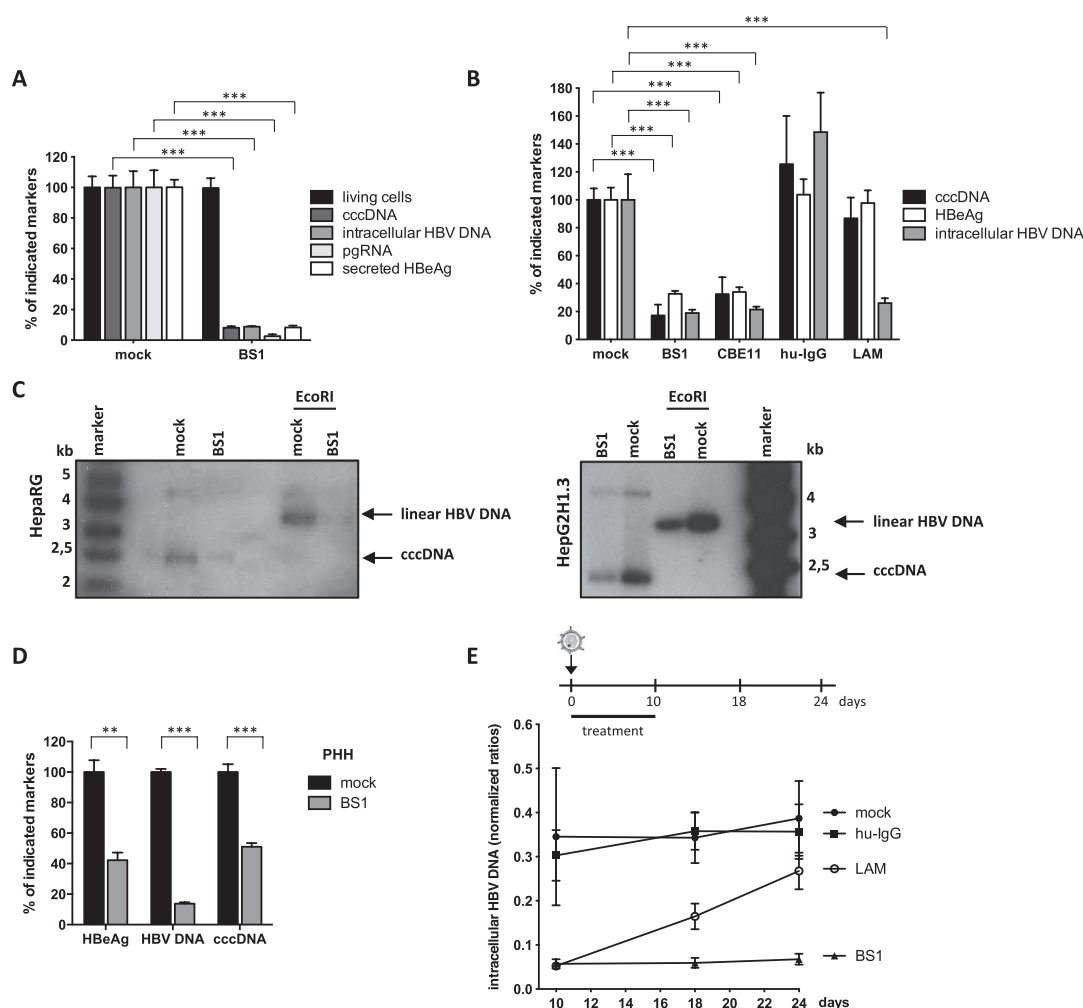
After cytidine deamination, DNA glycosylases recognize the damaged DNA and cleave N-glycosidic bonds to release the base and create an accessible apurinic/apyrimidinic site (AP site) that can then be cleaved by endonucleases (22).

These AP sites can be repaired, can lead to mutations upon DNA replication, or can induce DNA degradation (23). We quantified AP sites created by LT β R activation or IFN- α treatment. However, no increase of AP sites in total DNA extracts from dHepaRG cells or PHHs treated with IFN- α or LT β R agonists (fig. S8C) was found, indicating again that our treatments did not lead to detectable damage in genomic DNA. Because AP sites in the small (3.2 kb) cccDNA are very likely to be missed by this analysis, we digested total DNA extracts with an AP endonuclease (APE1) and then amplified cccDNA by qPCR. APE digestion further decreased cccDNA extracted from dHepaRG cells and PHHs treated with IFN- α or LT β R agonists but not with LAM (Fig. 3D). Taken together, our data indicate that both LT β R activation and IFN- α treatment induced deamination and AP site formation in HBV cccDNA, leading to its degradation, but did not affect genomic DNA.

LT β R Activation and IFN- α Treatment Up-Regulate Expression of Nuclear APOBEC3 Deaminases

IFN- α is known to induce several cytidine deaminases (23, 24). We performed genome-wide expression profiling of HBV-infected dHepaRG

Fig. 2. LT β R activation inhibits HBV infection and leads to cccDNA degradation in HepaRG cells and PHHs. (A and B) HBV-infected dHepaRG cells were treated with BS1, CBE11, human immunoglobulin (hu-IgG) control, or lamivudine (LAM). Treatment started 24 hours before infection for 12 days (A) or at 18 dpi for 10 days (B). Levels of the indicated HBV markers as well as cell viability are given relative to untreated controls (mock). (C) cccDNA levels were analyzed after 14 days of BS1 treatment by Southern blot in HBV-infected dHepaRG and HBV-replicating HepG2-H1.3 cells. Supercoiled cccDNA bands were identified by their expected size and linearization upon EcoRI digestion (3.2 kb). (D) PHHs were infected with HBV and treated with BS1 at 7 dpi for 10 days. Levels of the indicated HBV markers were compared to untreated PHHs of the same donor (donor 3) (mock). (E) HBV-infected dHepaRG cells were treated with BS1, hu-IgG control, or LAM. Intracellular HBV-DNA was analyzed 8 and 14 days after treatment cessation. Data are means \pm SD of replicates from independent experiments and were analyzed by *t* test. **P* < 0.05, ***P* < 0.01, ****P* < 0.001.



cells after LTβR activation (fig. S9A) and classified regulated genes according to their activity and properties (fig. S9B). The gene encoding APOBEC3B (A3B) was identified as the most up-regulated gene with nucleic acid-binding properties (fig. S9C). Analysis of all APOBEC3 family members showed that LTβR activation leads to strong up-

regulation of A3B, and to a lesser extent A3G, in HBV-infected dHepaRG cells and PHHs and after systemic application in human liver chimeric uPA-SCID mice (fig. S10A). A3B expression was induced by LTβR activation in a dose-dependent manner, and expression levels steadily increased during continuous treatment (fig. S11), correlating with a concomitant increase in treatment efficacy

over time (fig. S3C). Treatment of PHHs isolated from different donors with the LTβR agonist BS1 resulted in cccDNA degradation at different levels (Fig. 3E and fig. S10B), which could be explained neither by the difference in the level of A3B up-regulation (Fig. 3E) nor by detection of a previously described (25) genomic deletion of the A3B allele, which seems to correlate with

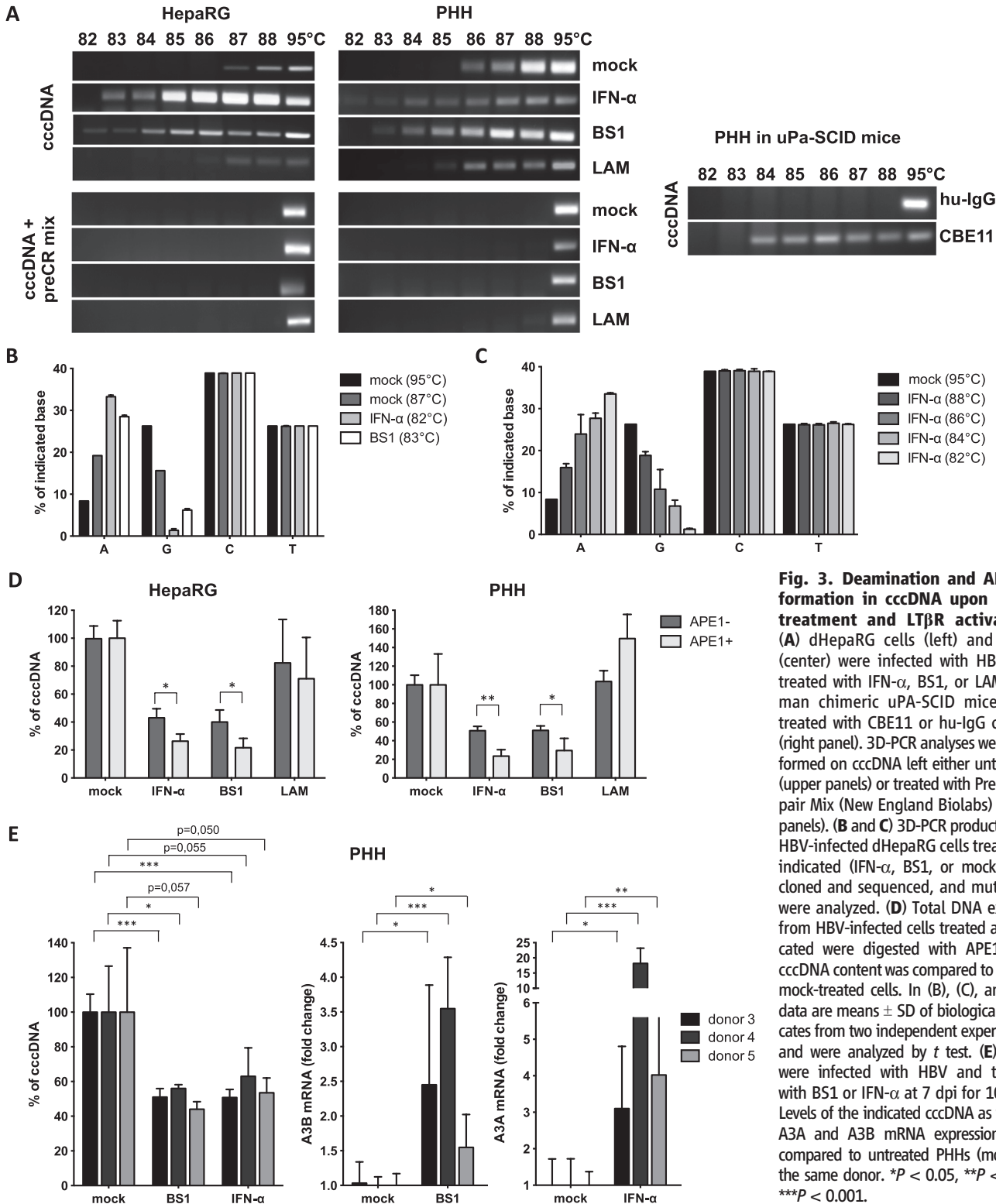


Fig. 3. Deamination and AP site formation in cccDNA upon IFN-α treatment and LTβR activation. (A) dHepaRG cells (left) and PHHs (center) were infected with HBV and treated with IFN-α, BS1, or LAM. Human chimeric uPA-SCID mice were treated with CBE11 or hu-IgG control (right panel). 3D-PCR analyses were performed on cccDNA left either untreated (upper panels) or treated with PreCR Repair Mix (New England Biolabs) (lower panels). (B and C) 3D-PCR products from HBV-infected dHepaRG cells treated as indicated (IFN-α, BS1, or mock) were cloned and sequenced, and mutations were analyzed. (D) Total DNA extracts from HBV-infected cells treated as indicated were digested with APE1, and cccDNA content was compared to that of mock-treated cells. In (B), (C), and (D), data are means ± SD of biological triplicates from two independent experiments and were analyzed by *t* test. (E) PHHs were infected with HBV and treated with BS1 or IFN-α at 7 dpi for 10 days. Levels of the indicated cccDNA as well as A3A and A3B mRNA expression were compared to untreated PHHs (mock) of the same donor. **P* < 0.05, ***P* < 0.01, ****P* < 0.001.

HBV persistence in infected patients (fig. S10, B and C).

In contrast to LT β R activation, IFN- α treatment induced mainly A3A expression, as well as A3F and A3G expression, in HBV-infected dHepaRG cells and PHHs (fig. S12A) and A3D expression in isolated PHHs. By systemic IFN treatment of chimpanzees (26), A3A was strongly up-regulated in liver needle biopsies (fig. S12B). Activation of A3A, A3F, and A3G after IFN- α treatment was dose- and time-dependent and decreased after an initial peak despite continuous treatment, indicating that cells become refractory to IFN- α (fig. S13). In patients treated with subcutaneous pegylated IFN- α , needle biopsies obtained at different time points confirmed a rapid, strong up-regulation of A3A (and, to a lesser extent, A3G) in the liver, peaking at 16 hours after treatment (fig. S12C). Expression levels declined after this time point and remained low until day 6 after treatment, confirming a fast but transient induction of A3A by IFN- α treatment. The findings that IFN- α induced a transient A3A induction and that cells

rapidly became refractory to IFN- α may account for the limited effect of IFN- α treatment in HBV-infected patients (3).

APOBEC3A or APOBEC3B Activity Is Essential to Induce cccDNA Degradation

Among the APOBEC3 family members up-regulated in our experiments, only A3A and A3B located to the nucleus (fig. S14), where they can gain access to cccDNA. To verify that they are indeed responsible for the induction of cccDNA degradation, we overexpressed the HIV-Vif protein [known to promote the degradation of all APOBEC3 proteins except A3B (27, 28)] in dHepaRG cells in a tetracycline-regulated fashion. Expression of HIV-Vif reduced A3A, A3F, and A3G expression (fig. S15A), reverted IFN- α -induced cccDNA deamination, and prevented cccDNA degradation induced by IFN- α treatment (Fig. 4A). However, expression of HIV-Vif did not alter A3B levels (fig. S15B) and had no impact on cccDNA degradation by LT β R activation (fig. S15C). To specifically address the role of

A3A or A3B in cccDNA degradation, we further knocked down A3A and A3B in dHepaRG cells under IFN- α or LT β R agonist treatment, respectively, and observed reduced cccDNA deamination (Fig. 4, B and C, left panels). Both A3A and A3B knockdown completely reverted cccDNA degradation but could not rescue the additional effect of IFN- α or LT β R activation on HBV replication (Fig. 4, B and C, right panels).

To confirm the impact of A3A and A3B on cccDNA deamination, we overexpressed A3A and A3B, respectively, in HBV-replicating HepG2-H1.3 cells (Fig. 4, D and E). Cytidine deamination of nuclear cccDNA by A3A and A3B is in accordance with other studies showing that both localize to the nucleus (29) and may be involved in the elimination of foreign DNA (23).

APOBEC3A Interacts with HBV Core Protein and Binds to cccDNA

APOBECs have evolved to restrict retroviral replication (30) as well as DNA transfer into cells. They are able to clear foreign nuclear DNA (23, 31),

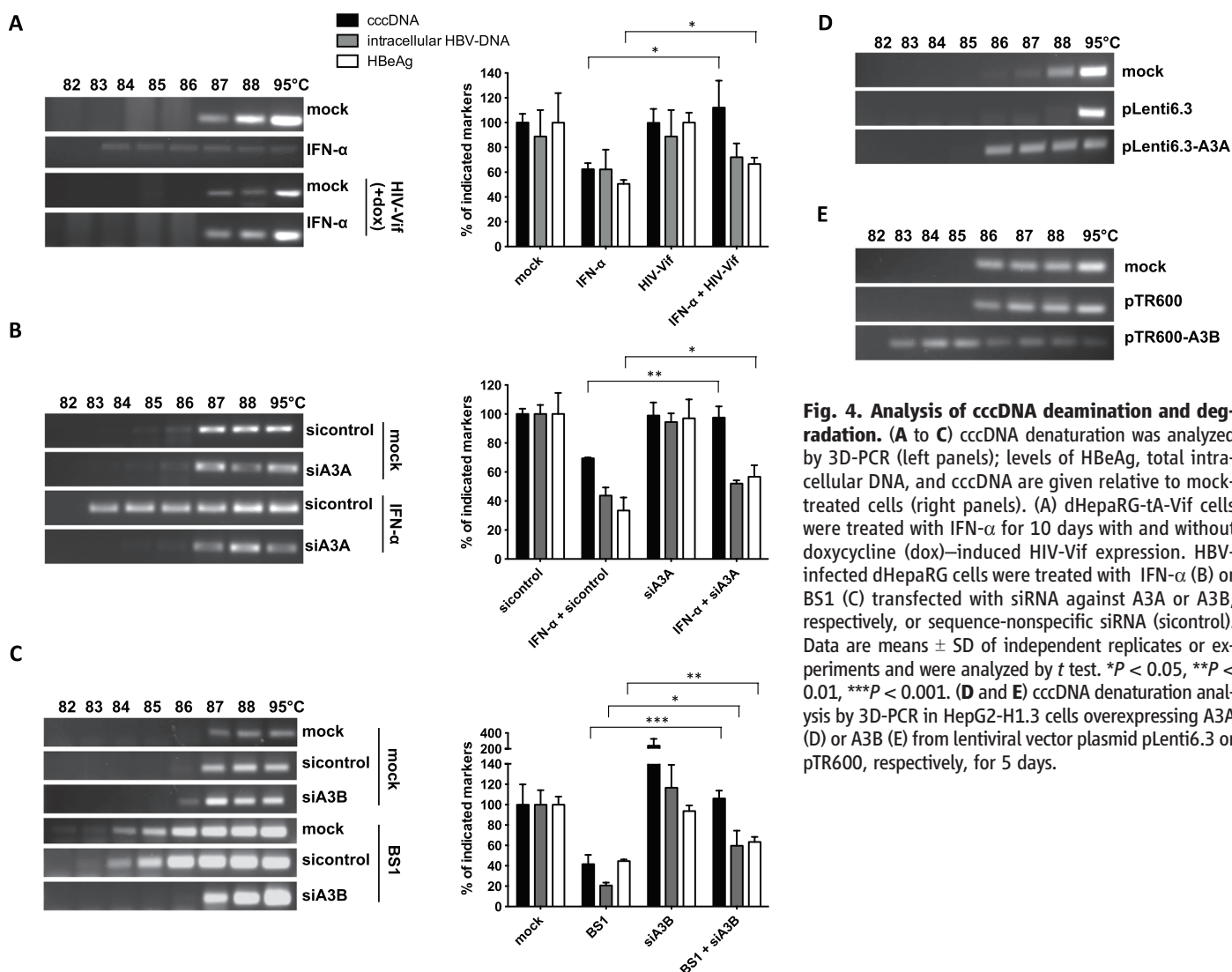


Fig. 4. Analysis of cccDNA deamination and degradation. (A to C) cccDNA denaturation was analyzed by 3D-PCR (left panels); levels of HBeAg, total intracellular DNA, and cccDNA are given relative to mock-treated cells (right panels). (A) dHepaRG-tA-Vif cells were treated with IFN- α for 10 days with and without doxycycline (dox)-induced HIV-Vif expression. HBV-infected dHepaRG cells were treated with IFN- α (B) or BS1 (C) transfected with siRNA against A3A or A3B, respectively, or sequence-nonspecific siRNA (sicontrol). Data are means \pm SD of independent replicates or experiments and were analyzed by *t* test. **P* < 0.05, ***P* < 0.01, ****P* < 0.001. (D and E) cccDNA denaturation analysis by 3D-PCR in HepG2-H1.3 cells overexpressing A3A (D) or A3B (E) from lentiviral vector plasmid pLenti6.3 or pTR600, respectively, for 5 days.

but it remains unclear how HBV cccDNA was recognized and whether it was specifically targeted in our experiments. To assess specificity, we generated cell lines replicating a mammalian replicon plasmid pEpi containing a linear HBV 1.3× overlength sequence. From the linear HBV genome, HBV replication was initiated and, in addition to the pEpi-H1.3 replicon, HBV cccDNA was established in the nucleus. Treatment with either IFN- α or the LT β R agonist BS1 inhibited HBV replication and resulted in deamination and degradation of HBV cccDNA, but not of the HBV sequence-containing replicon (fig. S16). This result indicated that the deamination and subsequent degradation induced by both treatments is HBV cccDNA-specific.

HBV core protein associates with A3G (32) and HBV cccDNA (33) and was thus a candidate to mediate the targeting of A3 deaminases to HBV cccDNA. Confocal microscopy indicated a colocalization of A3A and A3B with the HBV core in different cell lines and PHHs (Fig. 5 and fig. S17). Chromatin immunoprecipitation (ChIP) experiments using stably (fig. S18A) or transiently transfected HepG2-H1.3 cells or HBV-infected and IFN- α treated dHepaRG cells showed that HBV core protein and A3A both bind to the cccDNA minichromosome (Fig. 6A). Supporting the possibility that a guardian protein prevents A3A direct binding to DNA (34), we could not detect A3A binding to genomic DNA (fig. S18B) even in the presence of the HBV core, which has been reported to also bind to cellular DNA (35).

HBV core protein coimmunoprecipitated A3A in HepG2-H1.3 cells and transfected HuH7 cells, indicating physical interaction with A3A (fig. S19). Proximity ligation assay (PLA) (Fig. 6B and fig. S20) and fluorescence resonance energy transfer (FRET) analysis (Fig. 6C) confirmed that the HBV core expressed after HBV infection directly interacted with A3A induced by IFN- α . By deletion analysis, we determined that the central region of HBc (amino acids 77 to 149) is involved in the interaction with A3A (Fig. 6C and fig. S21).

These data suggest that A3A may be targeted to cccDNA by interaction with the HBV core. No such targeting to genomic DNA has been described so far. Because APOBEC3 deaminases are thought to act on single-stranded DNA (36), one possibility is that A3A and A3B act on cccDNA when it is transiently rendered into single-stranded form by RNA polymerase II before transcription initiation.

We therefore suggest the following mechanism of APOBEC-dependent degradation of HBV cccDNA (Fig. 6D). High-dose IFN- α treatment or LT β R activation up-regulate the expression of A3A and A3B, respectively, which subsequently colocalize or directly interact with HBV core in infected hepatocytes and then translocate to the nucleus, where they are brought into close contact with cccDNA by the HBV core. The APOBECs can now deaminate cccDNA that is transiently rendered single-stranded during transcription. Uracils in HBV cccDNA are recognized and ex-

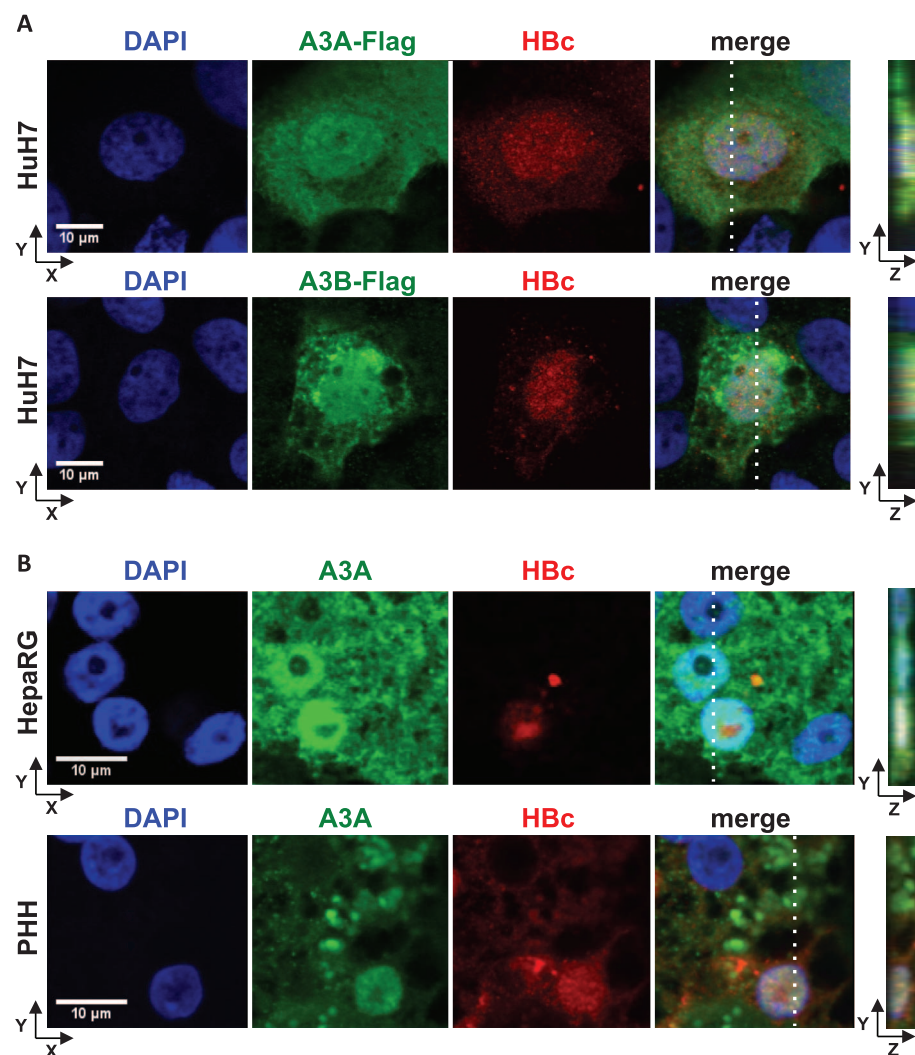


Fig. 5. Colocalization of A3A and A3B with HBV core protein (HBc). (A) HuH7 cells were co-transfected with an HBV 1.1× overlength genome and A3A-Flag- or A3B-Flag-expressing plasmids and stained using 4',6-diamidino-2-phenylindole (DAPI) and antibodies to HBc and Flag. (B) HBV-infected dHepaRG cells and PHHs were treated with IFN- α at 7 dpi for 3 days. A3A and HBc were analyzed by immunofluorescence staining. Right panels indicate Z stacks taken at the dotted lines.

cised by cellular DNA glycosylases, leading to the formation of AP sites, which are then recognized by cellular AP endonucleases (23), leading in turn to cccDNA digestion. Why cccDNA is degraded instead of being repaired by the cellular DNA repair machinery has remained elusive. Using a mixture of various enzymes, we were able to repair deaminated cccDNA in *tubo* (Fig. 3A); this suggests the induction of an additional factor promoting DNA degradation or an impaired function of the repair machinery, rather than a lack of recognition by the repair machinery. Thus, we can only speculate that either (i) the number of AP sites introduced after treatment is too high and exceeds the capacity of the cellular repair machinery, or (ii) IFN- α treatment or LT β R activation [or even HBV itself (37)] modulates the repair machinery. This may shift the equilibrium from cccDNA repair (38) to degradation.

Ideally, a cure for HBV infection needs to eliminate cccDNA. Therefore, cytokines or cytokine receptor agonists that can trigger HBV cccDNA deamination and its degradation are interesting antiviral candidates. Antivirals that induce A3A and/or A3B activity should be combined with nucleoside or nucleotide analogs to avoid the replenishment of nuclear cccDNA after degradation. LT β R agonists were active at low doses, and we did not observe any toxicity *in vitro* or *in vivo*, nor did we detect any modification of genomic DNA. Constitutive overexpression of LT α / β for more than 1 year has been associated with inflammatory liver disease and hepatocellular carcinoma (16). As antivirals, however, LT β R agonists would be used for only a limited period of time, minimizing the risk of side effects. Moreover, LT β R activation has already been explored as a cancer treatment (18).

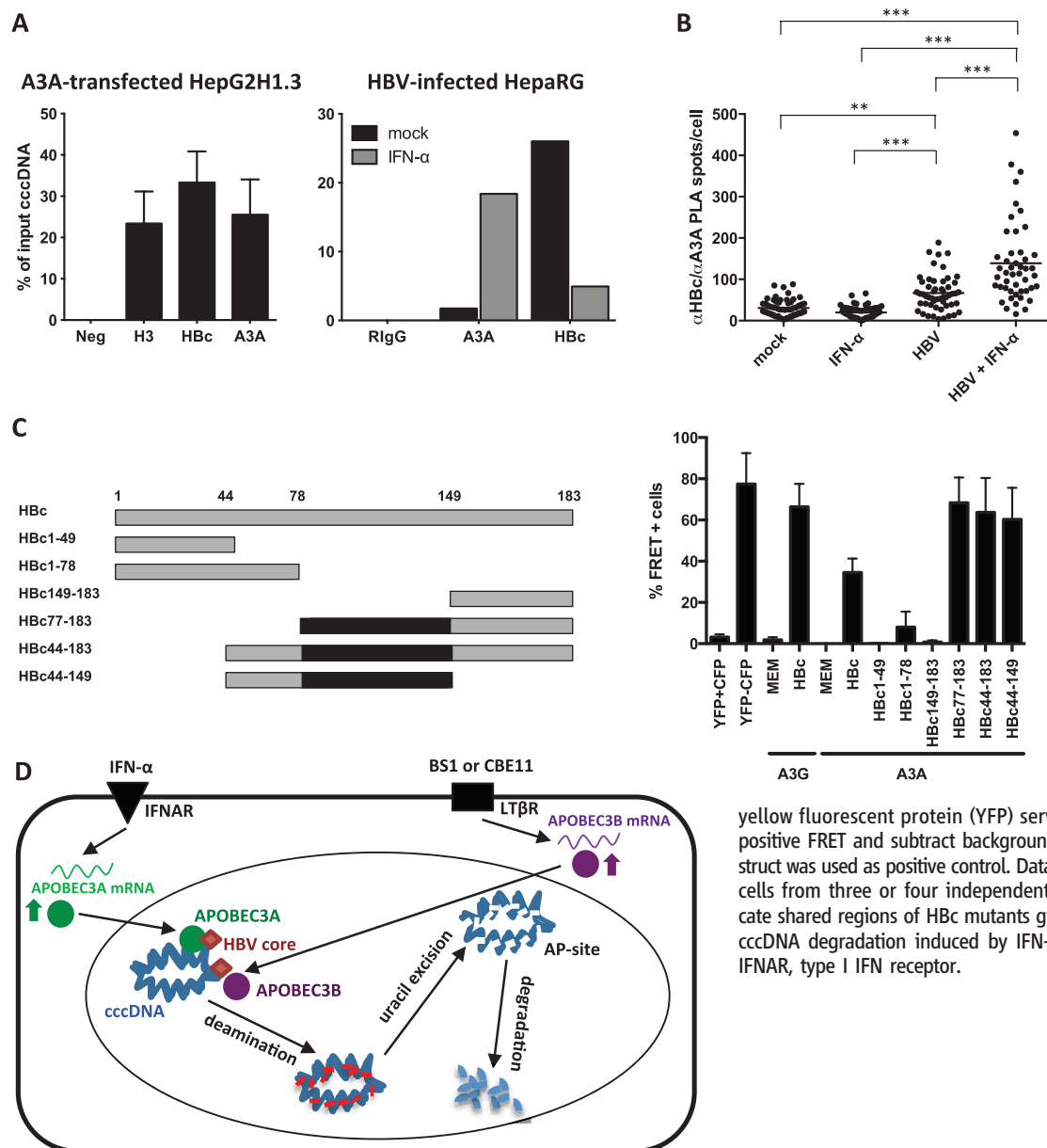


Fig. 6. Interaction of A3A, HBV core protein (HBc), and cccDNA. (A) Chromatin immunoprecipitation (ChIP) was performed using lysates of HepG2-H1.3 cells transfected with A3A-expressing plasmid or HBV-infected dHepaRG cells treated with IFN- α for 3 days. IPs using antibodies against histone H3, A3A, HBc, and control rabbit IgG (RlgG) were analyzed by qPCR for cccDNA. (B) Interaction between HBc and A3A was assessed by proximity ligation assay (PLA) in HBV-infected, IFN- α -treated dHepaRG cells. PLA spots were quantified in single cells by software-based spot counting. Data were analyzed by one-way analysis of variance. $^{**}P < 0.01$, $^{***}P < 0.001$. (C) Serial HBV core deletion mutants (left) were fused to cyan fluorescent protein (CFP), and interaction with A3A-YFP was assessed by fluorescence-activated cell sorting and FRET in HuH7.5 hepatoma cells (right). Cells cotransfected with CFP and yellow fluorescent protein (YFP) served as controls to exclude false positive FRET and subtract background signals. A CFP-YFP fusion construct was used as positive control. Data are means \pm SD of FRET-positive cells from three or four independent experiments. Black boxes indicate shared regions of HBc mutants giving a FRET signal. (D) Model of cccDNA degradation induced by IFN- α treatment or LT β R activation. IFNAR, type I IFN receptor.

cells cotransfected with CFP and yellow fluorescent protein (YFP) served as controls to exclude false positive FRET and subtract background signals. A CFP-YFP fusion construct was used as positive control. Data are means \pm SD of FRET-positive cells from three or four independent experiments. Black boxes indicate shared regions of HBc mutants giving a FRET signal. (D) Model of cccDNA degradation induced by IFN- α treatment or LT β R activation. IFNAR, type I IFN receptor.

A recent study has shown a higher frequency of an A3B deletion allele in persistent HBV carriers and hepatocellular carcinoma patients relative to healthy controls (25). This finding was further supported by the moderate deamination of cccDNA even in the absence of treatment, and by the observation that knockdown of A3B in the absence of any treatment increased cccDNA levels. Although deregulated expression of A3A and A3B has been shown to correlate with genomic DNA mutations (39, 40), we did not detect any alterations of genomic DNA using analyses of AP sites, 3D-PCR analysis, and deep sequencing of a set of human genes.

Our data indicate that cccDNA degradation is possible and can be induced without side effects on the infected host cell. An important task will be the testing of combinations of nucleoside or nucleotide analogs with novel antiviral strategies

[e.g., LT β R agonists or adoptive T cell therapy (41)] to activate A3A or A3B to cure hepatitis B.

References and Notes

- U. Protzer, M. K. Maini, P. A. Knolle, *Nat. Rev. Immunol.* **12**, 201–213 (2012).
- F. Zoulim, *Liver Int.* **31** (suppl. 1), 111–116 (2011).
- K. Wursthorn et al., *Hepatology* **44**, 675–684 (2006).
- L. G. Guidotti et al., *Proc. Natl. Acad. Sci. U.S.A.* **91**, 3764–3768 (1994).
- L. G. Guidotti et al., *Science* **284**, 825–829 (1999).
- S. F. Wieland, H. C. Spangenberg, R. Thimme, R. H. Purcell, F. V. Chisari, *Proc. Natl. Acad. Sci. U.S.A.* **101**, 2129–2134 (2004).
- H. McClary, R. Koch, F. V. Chisari, L. G. Guidotti, *J. Virol.* **74**, 2255–2264 (2000).
- L. Belloni et al., *J. Clin. Invest.* **122**, 529–537 (2012).
- A. Rang, S. Günther, H. Will, *J. Hepatol.* **31**, 791–799 (1999).
- V. Pasquetto, S. F. Wieland, S. L. Uprichard, M. Tripodi, F. V. Chisari, *J. Virol.* **76**, 5646–5653 (2002).
- S. F. Wieland, L. G. Guidotti, F. V. Chisari, *J. Virol.* **74**, 4165–4173 (2000).
- S. L. Uprichard, S. F. Wieland, A. Althage, F. V. Chisari, *Proc. Natl. Acad. Sci. U.S.A.* **100**, 1310–1315 (2003).
- P. Gripon et al., *J. Virol.* **62**, 4136–4143 (1988).
- P. Gripon et al., *Proc. Natl. Acad. Sci. U.S.A.* **99**, 15655–15660 (2002).
- M. J. Wolf, G. M. Selezniek, N. Zeller, M. Heikenwalder, *Oncogene* **29**, 5006–5018 (2010).
- J. Haybaeck et al., *Cancer Cell* **16**, 295–308 (2009).
- S. Jost, P. Turelli, B. Mangeat, U. Protzer, D. Trono, *J. Virol.* **81**, 10588–10596 (2007).
- M. Lukashev et al., *Cancer Res.* **66**, 9617–9624 (2006).
- X. Hu et al., *Carcinogenesis* **34**, 1105–1114 (2013).
- E. Dejardin et al., *Immunity* **17**, 525–535 (2002).
- R. Suspène et al., *Proc. Natl. Acad. Sci. U.S.A.* **102**, 8321–8326 (2005).
- J. I. Friedman, J. T. Stivers, *Biochemistry* **49**, 4957–4967 (2010).
- M. D. Stenglein, M. B. Burns, M. Li, J. Lengyel, R. S. Harris, *Nat. Struct. Mol. Biol.* **17**, 222–229 (2010).
- M. Bonvin et al., *Hepatology* **43**, 1364–1374 (2006).

25. T. Zhang *et al.*, *Hum. Mol. Genet.* **22**, 1262–1269 (2013).
26. Y. Huang *et al.*, *Gastroenterology* **132**, 733–744 (2007).
27. B. P. Doehle, A. Schäfer, B. R. Cullen, *Virology* **339**, 281–288 (2005).
28. G. Berger *et al.*, *PLOS Pathog.* **7**, e1002221 (2011).
29. H. Muckenfuss *et al.*, *J. Biol. Chem.* **281**, 22161–22172 (2006).
30. C. Münk, A. Willemsen, I. G. Bravo, *BMC Evol. Biol.* **12**, 71 (2012).
31. M. A. Carpenter *et al.*, *J. Biol. Chem.* **287**, 34801–34808 (2012).
32. P. Turelli, B. Mangeat, S. Jost, S. Vianin, D. Trono, *Science* **303**, 1829 (2004).
33. C. T. Bock *et al.*, *J. Mol. Biol.* **307**, 183–196 (2001).
34. M. M. Aynaud *et al.*, *J. Biol. Chem.* **287**, 39182–39192 (2012).
35. Y. Guo *et al.*, *BMC Genomics* **13**, 563 (2012).
36. H. C. Smith, R. P. Bennett, A. Kizilyer, W. M. McDougall, K. M. Prohaska, *Semin. Cell Dev. Biol.* **23**, 258–268 (2012).
37. T. H. Lee, S. J. Elledge, J. S. Butel, *J. Virol.* **69**, 1107–1114 (1995).
38. K. Kitamura *et al.*, *PLOS Pathog.* **9**, e1003361 (2013).
39. S. Landry, I. Narvaiza, D. C. Lindesty, M. D. Weitzman, *EMBO Rep.* **12**, 444–450 (2011).
40. M. B. Burns *et al.*, *Nature* **494**, 366–370 (2013).
41. K. Krebs *et al.*, *Gastroenterology* **145**, 456–465 (2013).

Acknowledgments: We thank R. Bester, T. Asen, K. Ackermann, K. Kappes, M. Feuerherd, R. Baier, R. Hillermann, U. Finkel, A. Krikoni, and F. Zhang for technical support; L. Terracciano for analysis of acute hepatitis patients; F. Chisari for HBV transgenic mice (HBV 1.3.32); T. Buch and O. Prazeres da Costa for help with array analysis and data discussions; L. Allweiss and A. Groth for help in generating and treating humanized uPA-SCID mice; and Siemens Healthcare Diagnostics for reagents. Supported by grants from Fédération Belge Contre le Cancer (E.D.), a European Research Council starting grant (LiverCancerMechanism) (M.H.), the German Research Foundation (SFB 841 to M.D., SFB TR 36 to M.H., and SFB TR 22), the Peter-Hans Hofschneider Foundation and the Helmholtz Alliances HAIT (U.P.), and PCCC (M.H.). We acknowledge the support of the nonprofit foundation HTCR, which holds human tissue on trust, making it broadly available for research on an ethical and legal basis. Patent application EP12006XXX has been filed at the European patent

office: “Lymphotoxin signaling activation and its downstream mediators eliminate HBV ccc DNA.” Microarray data have been submitted to the GEO database (www.ncbi.nlm.nih.gov/geo/) with accession number GSE46667. Human liver chimeric uPA-SCID mice were handled in accordance with protocols approved by the ethical committee of the city and state of Hamburg (permission number G12/015). Experiments with HBV-transgenic mice were performed in accordance with German legislation governing animal studies and the Principles of Laboratory Animal Care guidelines, NIH (55.1-1-54-2531.3-27-08). The study protocol for the animal experiment in fig. S12B was approved at the Southwest Foundation for Biomedical Research, San Antonio, TX (IACUC 869 PT, approved in 2004).

Supplementary Materials

www.sciencemag.org/content/343/6176/1221/suppl/DC1
Materials and Methods

Figs. S1 to S21

Table S1

References (42–62)

18 July 2013; accepted 5 February 2014

Published online 20 February 2014;

10.1126/science.1243462

REPORTS

Free-Standing Single-Atom-Thick Iron Membranes Suspended in Graphene Pores

Jiong Zhao,^{1,3} Qingming Deng,² Alicja Bachmatiuk,^{1,3,4} Gorantla Sandeep,¹ Alexey Popov,² Jürgen Eckert,^{1,5} Mark H. Rummeli^{3,6*}

The excess of surface dangling bonds makes the formation of free-standing two-dimensional (2D) metals unstable and hence difficult to achieve. To date, only a few reports have demonstrated 2D metal formation over substrates. Here, we show a free-standing crystalline single-atom-thick layer of iron (Fe) using in situ low-voltage aberration-corrected transmission electron microscopy and supporting image simulations. First-principles calculations confirm enhanced magnetic properties for single-atom-thick 2D Fe membranes. This work could pave the way for new 2D structures to be formed in graphene membranes.

The success and promise of atomically thin carbon—namely, graphene (1)—has triggered enormous enthusiasm for the study of other two-dimensional (2D) materials such as hBN, MoS₂, and MoSe₂ (2, 3). These 2D films are able to be reduced to atomically thin layers while still maintaining mechanical integrity, because they are layered structures where the bonding

within a layer is covalent whereas the interlayer bonding occurs through weak van der Waals interactions, thus allowing individual layers to be easily separated. With bulk metals, at first glance, the nature of metallic bonding and their 3D structure prohibit them from existing as a monoatomic layer. The only reports for atomically thin metallic layers, thus far, are heteroepitaxial structures in which the metal atoms bond with the underlying substrates (4, 5). On the other hand, because of nondirectional metallic bonding and the excellent plasticity of metals, at the nanoscale, one can build few-atom or even single-atom bridges (6, 7). Many single atomic metallic layers (e.g., Fe, Co, and Mn) are attractive due to their inherent magnetic properties. For the case of 2D Fe monolayers, the magnetic moment is expected to be 3.1 μ_B , which is markedly higher than its bulk counterpart (2.2 μ_B), and, in addition, 2D Fe should have a large perpendicular magnetic anisotropy (8). Hence, 2D magnets could be promising for magnetic recording media. Most of what is known about 2D magnets is based on theoretical investigations. These studies point to their magnetic properties being highly sensitive to their structure (9). Face-centered cubic (FCC) Fe and body-centered cubic (BCC) Fe ultrathin films have been grown on Cu, W, SiC, MgO, and other surfaces (9–13). However, these structures interact with the underlying substrate. Free-standing 2D metal films do not suffer from substrate-based influences, thus preserving coordination and electron confinement.

Experimental and theoretical works have focused on the interactions between graphene and single metal atoms (including Fe atoms) (14–16) or clusters (17). We show that porous graphene under electron-beam irradiation can be extended to enable Fe atoms and clusters to entirely seal small perforations in graphene and form a single atomic crystalline Fe layer.

In our in situ investigation, a low-voltage spherical aberration-corrected transmission electron microscopy (LVACTEM) operating with an acceleration voltage of 80 kV was employed (18). The graphene samples were grown by chemical vapor deposition (CVD) over Ni/Mo substrates (19). The as-produced monolayer graphene was then transferred on to standard lacey carbon (TEM) grids using an FeCl₃ etching solution to detach the graphene (20). The transferred samples typically consist of large areas of monolayer graphene in which some regions contain remnant material from the transfer process, including remnant Fe species from decomposed FeCl₃ (20). Under close inspection, pure Fe can be found as small nanocrystals forming on the surface of the graphene, as single atoms or small clusters at the edge of pores in clean graphene, or as 2D crys-

¹Leibniz-Institut für Festkörper- und Werkstoffforschung Dresden (IFW) Dresden, Institute of Complex Materials, P.O. Box 270116, D-01171 Dresden, Germany. ²IFW Dresden, Institute of Solid State Research, P.O. Box 270116, D-01171 Dresden, Germany. ³IBS Center for Integrated Nanostructure Physics, Institute for Basic Science (IBS), Daejeon 305-701, Republic of Korea. ⁴Centre of Polymer and Carbon Materials, Polish Academy of Sciences, M. Curie-Skłodowskiej 34, Zabrze 41-819, Poland. ⁵Technische Universität Dresden, Institute of Materials Science, 01062 Dresden, Germany. ⁶Department of Energy Science, Department of Physics, Sungkyunkwan University, Suwon 440-746, Republic of Korea.

*Corresponding author. E-mail: mark@rummeli.com

Specific and Nonhepatotoxic Degradation of Nuclear Hepatitis B Virus cccDNA

Julie Lucifora, Yuchen Xia, Florian Reisinger, Ke Zhang, Daniela Stadler, Xiaoming Cheng, Martin F. Sprinzl, Herwig Koppensteiner, Zuzanna Makowska, Tassilo Volz, Caroline Remouchamps, Wen-Min Chou, Wolfgang E. Thasler, Norbert Hüser, David Durantel, T. Jake Liang, Carsten Münk, Markus H. Heim, Jeffrey L. Browning, Emmanuel Dejaridin, Maura Dandri, Michael Schindler, Mathias Heikenwalder and Ulrike Protzer

Science **343** (6176), 1221-1228.

DOI: 10.1126/science.1243462 originally published online February 20, 2014

Clearance of Chronic Virus

The family of mRNA-editing enzymes, APOBEC, restricts hepatitis B virus (HBV) replication. **Lucifora *et al.*** (p. 1221, published online 20 February; see the Perspective by **Shlomai and Rice**) provide evidence that specific APOBECs mediate the anti-HBV effects of host cytokines, which in turn apparently induce nuclear deaminase activity without damaging host cells. Thus, there may be potential in these findings for developing a therapeutic route to curing chronic HBV infection.

ARTICLE TOOLS

<http://science.sciencemag.org/content/343/6176/1221>

SUPPLEMENTARY MATERIALS

<http://science.sciencemag.org/content/suppl/2014/02/19/science.1243462.DC1>

RELATED CONTENT

<http://science.sciencemag.org/content/sci/343/6176/1212.full>
<http://stm.sciencemag.org/content/scitransmed/2/32/32ra35.full>
<http://stke.sciencemag.org/content/sigtrans/7/317/ec73.abstract>
<http://science.sciencemag.org/content/sci/344/6189/1237.1.full>
<http://science.sciencemag.org/content/sci/344/6189/1237.2.full>

REFERENCES

This article cites 60 articles, 22 of which you can access for free
<http://science.sciencemag.org/content/343/6176/1221#BIBL>

PERMISSIONS

<http://www.sciencemag.org/help/reprints-and-permissions>

Use of this article is subject to the [Terms of Service](#)